

## Measurements of electrons from heavy flavor decays at the STAR experiment

---

**Katarina Gajdosova for STAR Collaboration\***

*Department of Physics*

*Faculty of Nuclear Sciences and Physical Engineering*

*Czech Technical University in Prague*

*Břehová 7, 115 19 Prague 1, Czech Republic*

*E-mail: [gajdokat@fjfi.cvut.cz](mailto:gajdokat@fjfi.cvut.cz)*

A hot and dense form of matter with deconfined quarks and gluons is called the quark-gluon plasma (QGP). The properties of this medium are being studied in ultrarelativistic heavy-ion collisions at the Relativistic Heavy Ion Collider (RHIC). One of the experimental probes that enable us to reveal the properties of the QGP are heavy quarks, such as  $c$  and  $b$ . Non-photonic electrons (NPE) that originate from semileptonic decays of  $D$  and  $B$  mesons can serve as a good proxy for heavy quarks. NPE in both p+p and Au+Au collisions are measured at RHIC. The p+p collisions are important as a baseline for the comparison with heavy-ion collisions and as a test of pQCD calculations. In Au+Au collisions the nuclear modification factor  $R_{AA}$  is measured, which is sensitive to the effects of QGP on heavy quark production. Also the measurements of azimuthal anisotropy parameter,  $v_2$ , are important to further study the interaction between the heavy quarks and the medium.

In this proceedings measurements of NPE in different collision systems and at different beam energies are presented. In p+p collisions at  $\sqrt{s} = 200$  GeV the invariant NPE spectra are shown in a wide transverse momentum range. In Au+Au collisions the results of  $R_{AA}$  and  $v_2$  at  $\sqrt{s_{NN}} = 200$  GeV are discussed, as well as the dependence of these variables on the collisional energy  $\sqrt{s_{NN}} = 39, 62.4$  and 200 GeV.

*53rd International Winter Meeting on Nuclear Physics,  
26-30 January 2015  
Bormio, Italy*

---

\*Speaker.

## 1. Introduction

Heavy quarks, charm ( $c$ ) and bottom ( $b$ ), are one of the most promising probes for the hot QCD medium created in later stages of ultrarelativistic heavy-ion collisions at RHIC and the LHC, called the Quark-Gluon Plasma (QGP). These quarks are created during the early stages of heavy-ion collisions from scatterings with large momentum transfer before the creation of the QGP. Therefore, their initial production is not affected by the QGP. However, the final distribution of particles composed of these heavy quarks is affected by the interaction between heavy quarks and the QGP.

Heavy quarks have been studied at the STAR experiment via measurements of open heavy flavor mesons through hadronic decay channels in p+p and Au+Au collisions at  $\sqrt{s_{NN}} = 200$  GeV [1], [2]. Also, measurements of heavy quarks confined in charmonia or bottomia were performed. Results on  $J/\psi$  production in Au+Au and Cu+Cu collisions at  $\sqrt{s_{NN}} = 200$  GeV are presented in [3] and  $\Upsilon$  measurements in d+Au and Au+Au collisions at  $\sqrt{s_{NN}} = 200$  GeV can be found in [4]. Studies reveal a clear sign of interaction of heavy quarks with the hot and dense medium.

Electrons from semi-leptonic decays of  $D$  and  $B$  mesons, the so-called non-photonic electrons (NPE), can serve as a good proxy for heavy quarks. Semileptonic decay channel of open heavy flavor mesons is also an interesting approach to the study of heavy quarks because of the ability of STAR detector to trigger on high  $p_T$  electrons. The STAR experiment has already seen a large suppression of electrons produced from semileptonic decays of heavy flavor mesons in central Au+Au collisions [5] and we discuss these results later on. The PHENIX experiment has also performed numerous studies of the heavy flavor quarks. Studies of NPE production in proton-proton collisions are important as a test of perturbative QCD calculations and also serve as a baseline for the studies of NPE spectra in heavy-ion collisions. Heavy flavor decay electrons were measured in p+p collisions at  $\sqrt{s} = 200$  GeV [6], [7] as well as in Cu+Cu and Au+Au collisions at  $\sqrt{s_{NN}} = 200$  GeV [8], [9]. Observation of dependence on system size was published in [10] and the Cold Nuclear Matter effects, such as Cronin effect, were studied in d+Au collisions at  $\sqrt{s_{NN}} = 200$  GeV [11], [12].

In heavy-ion collisions the nuclear modification factor  $R_{AA}$  is a variable sensitive to the effects of QGP on heavy quark production. It is defined as the ratio of particle production in heavy-ion collisions to particle production in proton-proton collisions scaled by the mean number of binary collisions:

$$R_{AA} = \frac{1}{\langle N_{bin} \rangle} \frac{dN_{AA}^2/dydp_T}{dN_{pp}^2/dydp_T}. \quad (1.1)$$

If  $R_{AA} = 1$ , a heavy-ion collision is just a superposition of multiple proton-proton collisions. If the nuclear modification factor is below unity, it indicates a suppression, which means that at given  $p_T$  and rapidity there are less particles produced in heavy-ion collisions compared to p+p collisions due to possible effects of Quark-Gluon Plasma.

The elliptic flow  $v_2$  is used to further study the interaction between heavy quarks and the medium. It is defined as the second parameter in the Fourier series of particle production in terms of azimuthal angle  $\varphi$  with respect to reaction plane:

$$\frac{dN}{d\varphi} \propto [1 + 2v_1 \cos \varphi + 2v_2 \cos(2\varphi) + \dots]. \quad (1.2)$$

## 2. Detector layout

The Solenoidal Tracker at RHIC (STAR), is one of the two detectors active at the Relativistic Heavy Ion Collider at the Brookhaven National Laboratory. The detector covers  $2\pi$  in azimuth and two units of pseudorapidity around mid-rapidity and is wrapped inside a solenoidal magnet, which has a field strength of 0.5 T.

The STAR detector is composed of various subdetectors, each of them fulfilling different task in the particle detection. The detector is shown in the Fig. 1 (left).

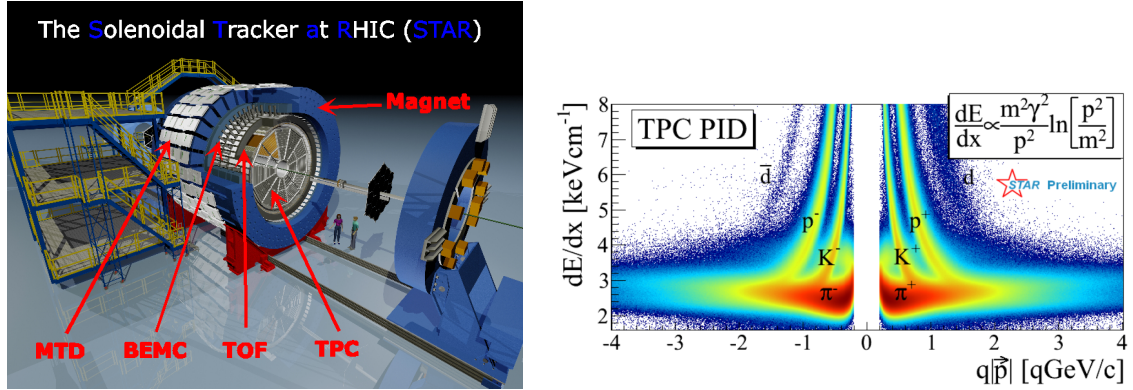


**Figure 1:** Left: View of the STAR detector. Right: Particle identification using TPC.

The main detector of the STAR is the so-called Time Projection Chamber (TPC), which is a gas detector designed for tracking and particle identification using their ionization energy loss in the gas as can be seen in Fig. 1 (right). The Time of Flight (ToF) detector is situated outside of the TPC. This detector is able to improve the particle identification at low  $p_T$  via the measurements of velocities of particles. The energy of electrons is obtained from the Barrel Electromagnetic Calorimeter (BEMC), which is outside of the ToF and also improves electron identification at high transverse momentum  $p_T$ .

The STAR detector was upgraded in the year 2014 with two new subdetectors. The Heavy Flavor Tracker (HFT) is situated in the center of STAR close to the beam pipe and will be able to directly measure the decay vertices of heavy flavor mesons, such as  $D$  and  $B$ . Outside of the magnet is the Muon Telescope Detector (MTD) designed for the detection of muons, as these are the only particles which pass through all the material of all subdetectors and the magnet. Using the MTD detector, the heavy flavor particles decaying into muons can be studied.

## 3. Analysis procedure

Non-photonic electrons originate in semileptonic decays of heavy flavor mesons. It is not possible to reconstruct the invariant mass of  $D(B)$  meson so we measure continuous spectrum. The contribution of background has to be subtracted.

The non-photonic electron yield is obtained according the following formula

$$N_{npe} = N_{inclusive} \epsilon_{purity} - N_{photonic} / \epsilon_{photonic}, \quad (3.1)$$

where  $N_{inc}$  is the inclusive electron yield,  $\varepsilon_{purity}$  is the purity of the electron yield,  $N_{photonic}$  is the photonic electron yield and  $\varepsilon_{photonic}$  is the photonic electron reconstruction efficiency. First, the inclusive electron sample is obtained and corrected with the purity for hadron contamination. Second, the background represented by photonic electrons has to be subtracted. Photonic electrons are those created in pairs  $e^+e^-$ . They come mainly from  $\gamma$  conversions or Dalitz decays. Only part of the pairs can be completely reconstructed. Therefore, the photonic electron yield needs to be corrected for the photonic electron reconstruction efficiency.

In order to obtain the purity of inclusive electron sample the normalized electron energy loss distribution is fitted with multi-Gaussian function at various  $p_T$  bins. Figure 2 (left) shows one  $p_T$  bin. The multi-Gaussian function is used due to hadron contamination, which is denoted in different colors in Fig. 2 (left). The dashed pink line represents  $\pi$ , the dot-dashed blue line  $K$ , the dashed red line are electrons, dot-dashed cyan color stands for protons and finally the dotted green line are the so called merged pions which are just wrongly reconstructed two tracks as one. The purity is then defined as the ratio of electron Gaussian to the multi-Gaussian within the  $n\sigma_e$  cut.

In Fig. 2 (right) the invariant mass of electron pairs at  $0.8 < p_T < 8.5$  GeV/c is shown. Electrons are paired with each other and grouped together according their charges. The unlike-sign distribution represents all  $e^+e^-$  pairs while like-sign distribution characterises the combinatorial background which is subtracted from the unlike-sign pairs. The resulting distribution contains the real photonic electrons as can be seen in Fig. 2 (right): only at low  $m_{ee}$  there are entries reflecting the low invariant mass of  $\gamma$  or  $\pi^0$ ,  $\eta$  Dalitz decays.

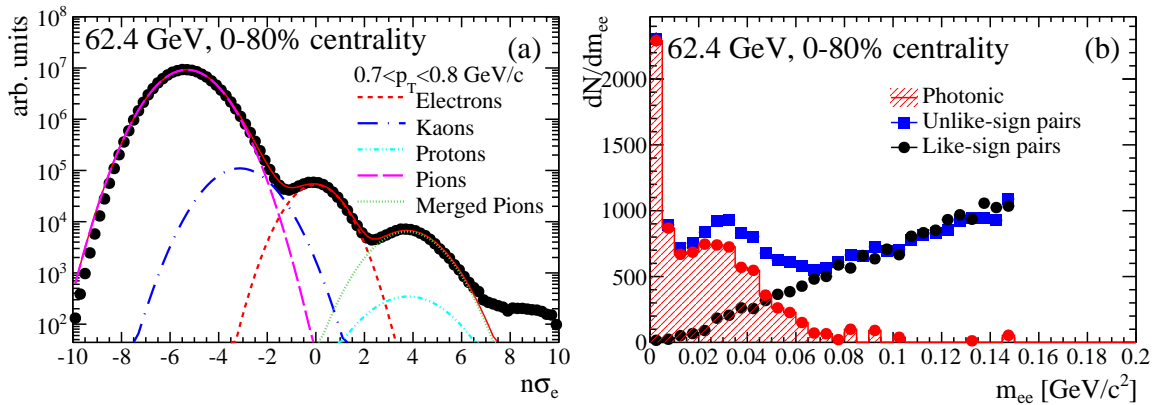


**Figure 2:** Left: Electron energy loss distribution. Taken from ref. [13]. Right: Invariant mass of electron pairs. Taken from ref. [13].

#### 4. p+p collisions at $\sqrt{s} = 200$ GeV

The invariant yield of non-photonic electrons in proton-proton collisions at  $\sqrt{s} = 200$  GeV is important as a test of perturbative QCD calculations. In Fig. 3 (left) the invariant yield of NPE is plotted as a function of transverse momentum  $p_T$ . Published STAR data from year 2008 [14] and published PHENIX results from year 2005 [6] are drawn in Fig. 3 together with the preliminary results of STAR from years 2009 and 2012. In the first case the NPE spectra were extended towards lower  $p_T$  and the latter analysis results were obtained up to  $p_T = 14$  GeV/c. However, in Fig. 3 the

spectra are drawn only up to  $p_T = 8 \text{ GeV}/c$  for better comprehensibility. On the same plot the data are compared to the theoretical calculations of Fixed Order Next-to-Leading Logarithm (FONLL) of pQCD [15].

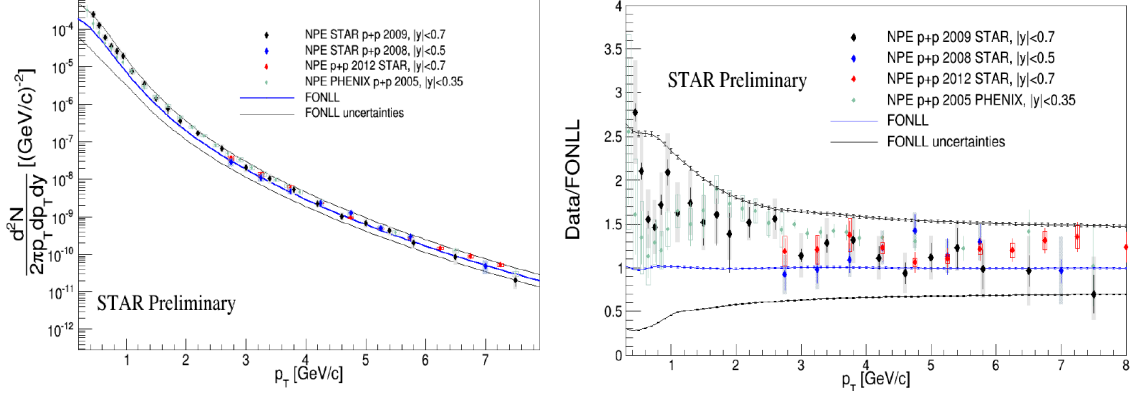


**Figure 3:** Left: Invariant yield of non-photonic electrons compared to FONLL pQCD calculations from ref. [15]. Published STAR data from year 2008 [14], PHENIX results from year 2005 [6], as well as the preliminary STAR results from years 2009 and 2012 are shown. Right: Ratio of measured invariant yield of non-photonic electrons to FONLL pQCD theoretical calculations. Taken from ref. [14], [6], [15].

The data agree well with each other and are consistent with the FONLL pQCD calculations within their uncertainties. This can be seen in Fig. 3 (right) where the ratio of the data to FONLL calculations is shown [14].

## 5. Au+Au collisions at $\sqrt{s_{NN}} = 200 \text{ GeV}$

The nuclear modification factor  $R_{AA}$  as defined above can reveal the effects of QGP on the particle production. At 0-10 % central Au+Au collisions at the energy of  $\sqrt{s_{NN}} = 200 \text{ GeV}$  the STAR experiment observes a strong suppression of non-photonic electrons at high  $p_T$  (Fig. 4 left). The  $R_{AA}$  is also compared to theoretical models based on different types of energy loss of heavy quarks inside the QGP.

The DGLV Rad. model [16] marked with dashed green line considers only gluon radiation energy loss mechanism and does not describe the suppression at high  $p_T$ . A DGLV model which includes in addition the collisional energy loss (DGLV Rad. + El.) predicts larger suppression compared to the previous one. The non-perturbative approach to quark energy loss presented by He *et al.* [17] is marked with magenta line. The BAMPS partonic transport model [18], [19] marked with black dashed line calculates the quark energy loss due to elastic collisions with the medium. A collisional dissociation model represented by the red line uses the energy loss caused by the dissociation of heavy mesons in the strongly interacting medium [20]. This model, together with the AdS/CFT model [21], agree well with the data at high  $p_T$ . Finally, the model described by Gossiaux *et al.* [22], [23] calculates the radiative and collisional energy loss using pQCD description with non-perturbative corrections.

The measurement of elliptic flow of NPE in Au+Au collisions at  $\sqrt{s_{NN}} = 200 \text{ GeV}$  is shown in Fig. 4 (right). The  $v_2$  variable was obtained using 2-particle correlations  $v_2\{2\}$  or 4-particle

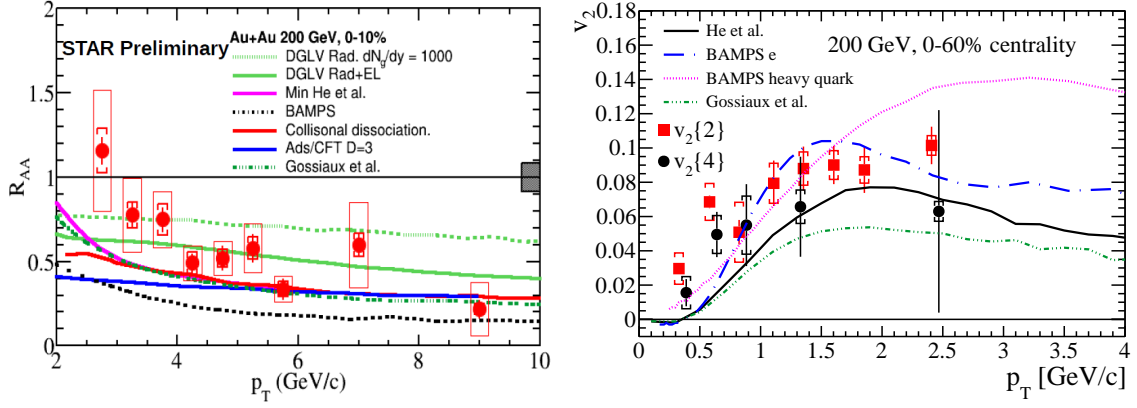


**Figure 4:** Left: The nuclear modification factor of non-photonic electrons in Au+Au collisions at  $\sqrt{s_{NN}} = 200$  GeV compared to models from ref. [16], [17], [18], [19], [20], [21], [22], [23]. Right: The elliptic flow of non-photonic electrons in Au+Au collisions at  $\sqrt{s_{NN}} = 200$  GeV compared to models. Taken from ref. [13], [17], [18], [19], [22], [23].

correlations  $v_2\{4\}$  [24]. A finite  $v_2$  is observed at low  $p_T$  which indicates strong in-medium interactions of heavy quarks [13]. Increasing  $v_2$  at high  $p_T$  can be described by jet-like correlations that are also present in p+p collisions. The measurements of elliptic flow are compared to the same theoretical models as is the  $R_{AA}$  [17], [18], [19], [22], [23]. In general, models which are able to reproduce the azimuthal anisotropy do not describe well the nuclear modification factor.

## 6. Au+Au collisions at $\sqrt{s_{NN}} = 39, 62.4$ GeV

In Au+Au collisions at lower beam energies of  $\sqrt{s_{NN}} = 62.4$  GeV the NPE measurements are not suppressed. The preliminary results on  $R_{AA}$  of NPE at the energy of  $\sqrt{s_{NN}} = 62.4$  GeV are shown in Fig. 5 (left). The Au+Au NPE yield was divided by the spectra calculated theoretically using pQCD [25]. The PHENIX experiment revealed the same pattern of  $R_{AA}$  of heavy flavor electrons at this beam energy [26]. The enhancement of nuclear modification factor can be caused by Cold Nuclear Matter effects (e.g. the Cronin effect), which seems to be more significant at lower beam energies and need to be studied in the future.

The azimuthal anisotropy using 2-particle correlations  $v_2\{2\}$  was also measured at low beam energies of  $\sqrt{s_{NN}} = 39, 62.4$  GeV, which can be seen in Fig. 5 (right). While the elliptic flow  $v_2$  at  $\sqrt{s_{NN}} = 200$  GeV has positive values, at lower collisional energies it is consistent with zero up to  $p_T = 1.6$  GeV/c. The difference between energy  $\sqrt{s_{NN}} = 200$  GeV and the lower beam energies are statistically significant [13].

## 7. Conclusions

In this proceedings the recent STAR results of electrons originating from decays of open heavy flavor mesons were discussed. First, the NPE spectra in p+p collisions at  $\sqrt{s} = 200$  GeV were shown and compared to theoretical predictions of FONLL pQCD calculations. The data from different years agree with each other as well as with the PHENIX results and FONLL calculations

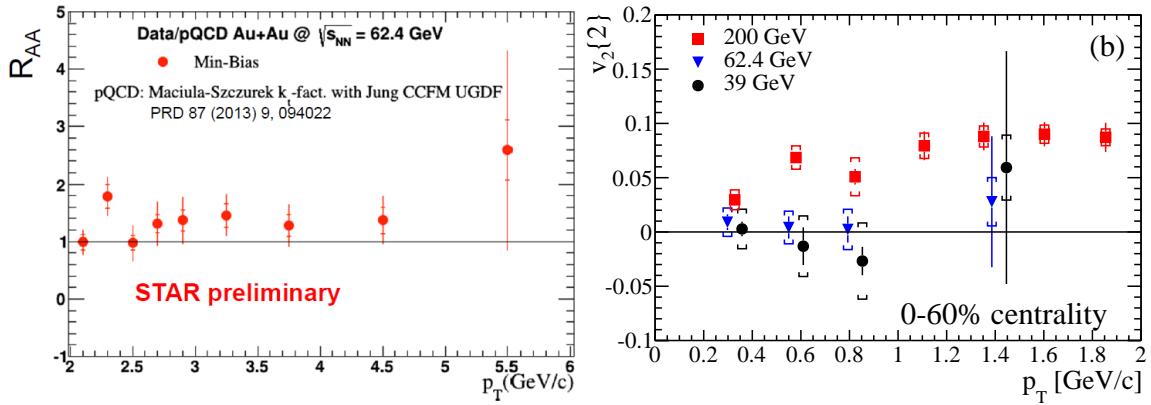


**Figure 5:** Left: The nuclear modification factor of non-photonic electrons in Au+Au collisions at  $\sqrt{s_{NN}} = 62.4$  GeV. The baseline was calculated theoretically using pQCD from ref. [25]. Right: The elliptic flow of non-photonic electrons in Au+Au collisions at  $\sqrt{s_{NN}} = 39, 62.4, 200$  GeV. Taken from ref. [13].

within uncertainties. Second, the preliminary results of nuclear modification factor at 0-10% central Au+Au collisions at  $\sqrt{s_{NN}} = 200$  GeV was shown and compared to various models. The data reveal strong suppression at high  $p_T$ . The comparison with models shows that heavy quarks lose energy in QGP not only through gluon radiation. Also, the elliptic flow  $v_2$  was presented and compared with the same models. Models which describe the  $R_{AA}$  are not able to reproduce the azimuthal anisotropy. Finally, the measurements of NPE at lower collisional energies  $\sqrt{s_{NN}} = 39, 62.4$  GeV were presented. The nuclear modification factor in Au+Au collisions at  $\sqrt{s_{NN}} = 62.4$  GeV was shown with no indication of suppression. These observations demonstrate that Cold Nuclear Matter effects could be more significant at these energies. The elliptic flow at  $\sqrt{s_{NN}} = 39$  and 62.4 GeV presented in this proceedings was consistent with 0.

The STAR experiment has been recently upgraded with two new detectors Heavy Flavor Tracker (HFT) and Muon Telescope Detector (MTD) which will help to improve the heavy flavor measurements. The HFT [27] will be able to reconstruct the decay vertices of  $D$  and  $B$  mesons. The studies of heavy flavor measurements via muon decay channels will be available using the MTD detector ( $|\eta| < 0.5$ ) [28].

## Acknowledgements

This work was supported by Grant Agency of the Czech Technical University in Prague, grant No. SGS13/215/OHK4/35/14 and by Grant Agency of the Czech Republic, grant No. 13-20841S.

## References

- [1] L. Adamczyk *et al.* (STAR Collaboration), Phys. Rev. D **86**, 072013 (2012).
- [2] L. Adamczyk *et al.* (STAR Collaboration), Phys. Rev. Lett. **113**, 142301 (2014).
- [3] L. Adamczyk *et al.* (STAR Collaboration), Phys. Rev. C **90**, 024906 (2014).
- [4] L. Adamczyk *et al.* (STAR Collaboration), Phys. Lett. B **735**, 127 (2014).

- [5] B. I. Abelev *et al.* (STAR Collaboration), Phys. Rev. Lett. **98**, 19301 (2007); Erratum-ibid. **106**, 159902 (2011).
- [6] A. Adare *et al.* (PHENIX Collaboration), Phys. Rev. Lett. **97**, 252002 (2006).
- [7] A. Adare *et al.* (PHENIX Collaboration), Phys. Rev. Lett. **103**, 082002 (2009).
- [8] A. Adare *et al.* (PHENIX Collaboration), Phys. Rev. C **86**, 024909 (2012).
- [9] A. Adare *et al.* (PHENIX Collaboration), Phys. Rev. Lett. **98**, 172301 (2007).
- [10] A. Adare *et al.* (PHENIX Collaboration), Phys. Rev. C **90**, 034903 (2014).
- [11] A. Adare *et al.* (PHENIX Collaboration), Phys. Rev. Lett. **109**, 242301 (2012).
- [12] A. Adare *et al.* (PHENIX Collaboration), Phys. Rev. Lett. **112**, 252301 (2014).
- [13] L. Adamczyk *et al.* (STAR Collaboration), arXiv: 1405.6348 [hep-ex] (2014).
- [14] H. Agakishiev *et al.* (STAR Collaboration), Phys. Rev. D **83**, 052006 (2011).
- [15] A.D. Frawley, T. Ullrich and R. Vogt, Phys. Rept. 462:125-175 (2008).
- [16] M. Djordjevic, M. Gyulassy, R. Vogt and S. Wicks, Phys. Lett. B **632**, 81 (2006).
- [17] M. He, R. J. Fries and R. Rapp, Phys. Rev. C **86**, 014903 (2012).
- [18] J. Uphoff, O.Fochler, Z. Xu and C. Greiner, Phys. Rev. C **84**, 024908 (2011).
- [19] J. Uphoff, O.Fochler, Z. Xu and C. Greiner, Phys. Lett. B **717**, 430 (2012).
- [20] R. Sharma, I. Vitev and B.-W. Zhang, Phys. Rev. C **80**, 054902 (2009).
- [21] W. Horowitz, AIP Conf. Proc. **1441**, 889-891 (2012).
- [22] P. Gossiaux and J. Aichelin, Phys. Rev. C **78**, 014904 (2008).
- [23] P. Gossiaux, J. Aichelin, T. Gousset and V. Guiho, J. Phys. G **37**, 094019 (2010).
- [24] N. Borghini, P. M. Dinh and J.-Y. Ollitrault, Phys.Rev. C **63**, 054906 (2001).
- [25] R. Maciula and A. Szczurek, Phys. Rev. D **87**, 094022 (2013).
- [26] A. Adare *et al.* (PHENIX Collaboration), arXiv: 1405.3301[nucl-ex] (2014).
- [27] E. Anderssen *et al.*, A Heavy Flavor Tracker for STAR:  
<http://www.osti.gov/scitech/servlets/purl/939892>.
- [28] L. Ruan *et al.*, STAR Muon Telescope Detector Proposal:  
[http://www.star.bnl.gov/~ruanlj/MTDreview2010/MTD\\_proposal\\_v14.pdf](http://www.star.bnl.gov/~ruanlj/MTDreview2010/MTD_proposal_v14.pdf).